http://dx.doi.org/10.5012/bkcs.2012.33.12.4093

Improvement in Long-Term Stability and Photovoltaic Performance of UV Cured Resin Polymer Gel Electrolyte for Dye-Sensitized Solar Cell

Geun Woo Park, Chul Gyun Hwang,† Jae Won Jung,‡ and Young Mee Jung*

*Department of Chemistry, and Institute for Molecular Science and Fusion Technology, Kangwon National University, Chunchon 200-701, Korea. *E-mail: ymjung@kangwon.ac.kr*
†Department of R&D, Nano Convergence Practical Application Center, Daegu 704-330, Korea
‡KENSCO, Deagu 704-240, Korea
Received August 21, 2012, Accepted September 22, 2012

We introduced a new UV-cured resin polymer gel as an electrolyte for dye-sensitized solar cells (DSSCs) that is cured with UV irradiation to form a thin film of UV-cured resin polymer gel in the cells. The gel film was characterized and its potential for use as an electrolyte in DSSCs was investigated. This new UV-cured resin polymer gel was successfully applied as a gel polymer electrolyte in DSSCs overcoming the problems associated with the liquid electrolytes in typical DSSCs. The effect of γ-butylrolactone (GBL) on the long-term stability and photovoltaic performance in DSSCs using this UV-cured resin polymer gel electrolyte was also investigated. The results of the energy conversion efficiency, ionic conductivity and Raman spectra of the UV-cured resin polymer gel electrolyte with the addition of 6 wt % GBL to the UV-cured resin polymer electrolyte showed good long-term stability and photovoltaic performance for the DSSCs with the UV-cured polymer gel electrolyte.

Key Words : UV-cured resin polymer gel, Electrolytes, Dye-sensitized solar cells (DSSCs), γ-Butylrolactone (GBL), Raman spectroscopy

Introduction

Dye-sensitized solar cells (DSSCs) have recently received considerable attention as a possible candidate for next-generation solar cells because of their potential of low cost, energy consumption, color choice, and transparency levels compared to conventional silicon-based solar cells.[1-6] However, DSSCs using liquid electrolytes have major issues with leakage and evaporation of the solvent, resulting in poor long-term stability. The long-term stability of DSSCs is essential for the practical use of these devices.[7-10] In other to overcome this problem, the liquid electrolyte has been replaced by room-temperature ionic liquids,[11,12] organic and inorganic hole-transport materials,[13-15] and polymer and gel electrolytes.[16-21] Among these methods, the DSSCs using polymer gel electrolytes have shown better performances when compared with the same device assembled with classical polymer electrolytes.[22-24] However, the overall conversion efficiency is still low in comparison to DSSCs fabricated using liquid electrolytes. This problem is attributed to the low ionic diffusion in more viscous media, limiting the photocurrent and resulting in low penetration depth of the polymer inside the nanostructured electrode and increased interfacial charge-transfer resistance between the electrode, and the electrolyte.[25] To help improve the overall conversion efficiency and transport properties in these devices, polymer gel systems have been modified with an additive material.[26-28] γ-Butylrolactone (GBL) has become a common additive in the polymer gel electrolytes because of its improvement of the ionic conductivity properties of these systems.[21,29]

In this study, we demonstrated a new UV-curable resin polymer gel, its characterization and its potential as an electrolyte in DSSCs. It can be cured with UV irradiation to form a thin film of a UV-curable resin polymer gel in the cells. The effect of GBL in terms of the long-term stability and photovoltaic performance of DSSCs using this UV-curable resin polymer gel electrolyte was also investigated.

Material and Methods

1,2-Dimethyl-3-propyl imidazolium iodide (DMPII), LiI, 4-*tert*-butylpyridine (TBP), acetonitrile, 1,6-hexanediol diacrylate, and GBL were purchased from Sigma Aldrich at the highest purity available. I_2 and hydroxycyclohexyl-phenyl-ketone were purchased from DukSan and Shinyoung Rad. Chem. Ltd., respectively, at the highest purity available. TiO_2 paste was purchased from Dyesol. All chemicals were used as received without further purification.

The liquid electrolyte consisted of DMPI, LiI, I_2, TBP, and acetonitrile, with an acetonitrle/TBP ratio of 8:2. The UV-cured resin consisted of a monomer (1,6-hexanediol diacrylate) and a photoinitiator (hydroxycyclohexyl-phenyl-ketone). The resin polymer electrolyte was prepared by mixing the liquid electrolyte and UV resin (50:50). GBL was added in order to improve the ionic conductivity of the UV-cured resin polymer electrolyte.

A porous TiO_2 film with a 12 mm thickness was formed on fluorine-doped tin oxide (FTO)-coated glass substrates *via* a screen-printing method. The TiO_2 films were then sensitized with a Ru-dye (N719, Dyesol) for 24 h.

DSSCs with a UV-cured resin polymer gel were fabricated with a TiO_2 electrode and the Pt counter electrode. The resin polymer electrolyte was introduced slowly into the cell through the gap between the TiO_2 porous film electrode and the Pt electrode, thereby integrating into the pores of the dye-sensitized TiO_2 nanostructured electrode. After UV irradiation, the resin polymer electrolyte was cured forming a thin film of UV-cured resin polymer gel in the cell.

Current-voltage (*I-V*) curves were measured using commercial solar cell efficiency & reliability equipment (Mac Science) by illuminating the cell through the active photoelectrode with a standard AM 1.5G optical filter. The power of the incident white light from the Xenon lamp was 100 mW/cm^2.

The ionic conductivities of the UV-cured resin polymer electrolytes in the DSSCs were measured with an Orion star series meter (KB-250, Thermo Scientific).

The diffusion coefficients (D_{app}) were determined by the following equation[30]

$$J_{\text{lim}} = \frac{2nFC_0D_{app}}{d} \quad (1)$$

where, n is the number of electrons per electroactive molecule, C_0 is the bulk concentration of the electroactive species, F is Faraday's constant, d is the distance between the electrodes, and J_{lim} is the diffusion limited currents.

Raman spectra were measured using a Jobin Yvon/ HORIBA LabRam ARAMIS Raman spectrometer equipped with an integral BX 41 confocal microscope. The radiation from an air-cooled frequency-doubled Nd:Yag laser (532 nm) was used as the excitation source. Raman scattering was detected with a 180° geometry using a multi channel air-cooled (−70 °C) charge-coupled device (CCD) camera (1024 × 256 pixels).

Results and Discussion

Figure 1 shows photos taken during the process of UV curing of the resin polymer gel electrolyte for a DSSC. After UV irradiation, the UV-curable polymer electrolyte was cured, and a thin film of the UV-cured resin polymer gel was clearly observed, as shown in Figure 1. This UV-cured resin polymer gel was successfully used as a gel polymer electrolyte in DSSCs to overcome the problems associated with liquid electrolytes in these devices.

To improve the long-term stability and photovoltaic performance of DSSCs using this UV-curable resin polymer gel electrolyte, GBL was added to the resin polymer electrolyte. Figure 2 shows a plot of the ionic conductivities of gel polymer electrolytes with different concentrations of GBL. The ionic conductivity of the gel polymer electrolytes increased significantly up to 6 wt % GBL and then slightly decreased. This indicates that the addition of 6 wt % GBL to the resin polymer electrolyte results in the greatest ionic conductivity. We can therefore expect that the highest energy conversion efficiency of DSSCs containing this additive and resin polymer electrolyte will occur with 6 wt % GBL.

We calculated the diffusion coefficient (D_{app}) of the UV-curable resin polymer gel electrolyte with different GBL concentrations according to Eq. (1). Figure 3 shows plots of the diffusion coefficients of UV-curable resin polymer gel electrolyte as a function of GBL concentration before and after UV curing. For without GBL, the diffusion coefficient of the UV-curable resin polymer gel electrolyte itself decreases after UV curing process. As the ionic conductivity increased with GBL concentration, as shown in Figure 2, the diffusion coefficients with the GBL additive tended to be greater after UV curing than the liquid polymer electrolyte without GBL. The highest diffusion coefficient value obtained with the addition of 8 wt % GBL. This occurs alongside the highest values of the short-circuit current density (J_{sc}) and open-circuit voltage (V_{oc}) observed for our DSSCs with

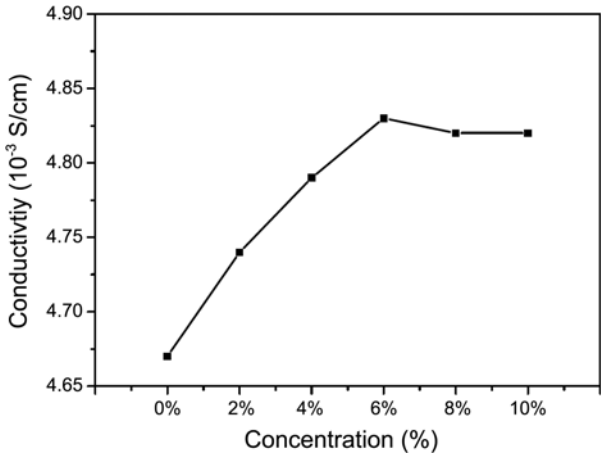

Figure 2. Plot of the ionic conductivities of UV-cured resin electrolytes with various GBL concentrations.

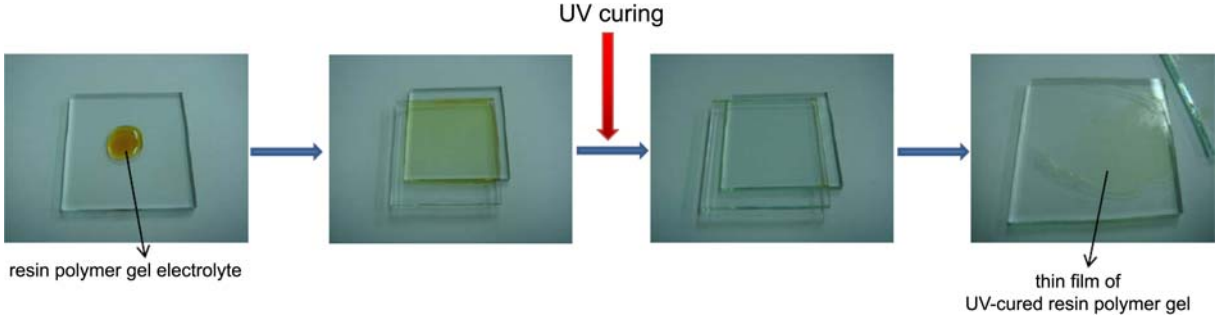

Figure 1. Photos taken during the process of UV cured the resin electrolyte for the DSSC cell.

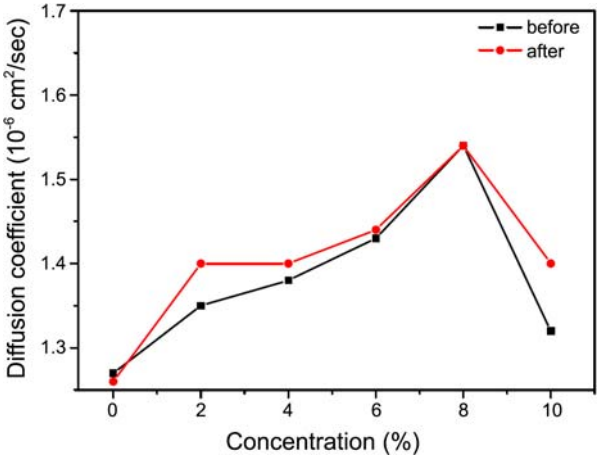

Figure 3. Plots of the diffusion coefficients for UV-cured resin electrolytes with different GBL concentrations before and after UV curing.

an 8 wt % GBL concentration. It can be found that values of the diffusion coefficient of the gel polymer electrolytes increased as the content of GBL increased up to 8 wt %. However, when the content of GBL exceeded 8 wt %, the diffusion coefficient of the gel polymer electrolytes decreased, with the ionic conductivity remaining almost the same. From the ionic conductivity and diffusion coefficient results, we can conclude that the optimum conditions for enhancement of both the ionic conductivity and diffusion coefficient of the gel polymer electrolytes occurs with the addition of 6-8 wt % GBL.

To better understand the effect of the ionic conductivity of the UV-curable resin polymer electrolyte on the overall efficiency of the DSSCs, we measured the Raman spectra for electrolytes with varying concentrations of GBL. Figure 4 shows the Raman spectra with increasing GBL concentrations. The inserted of Figure 4 is the Raman spectra of an enlarged region of the triiodide (I_3^-) species. The intensity of the prominent band observed at 115 cm^{-1}, which is assigned to I_3^-, increased with increasing GBL concentration. The trend in the spectral changes of the Raman spectra of the

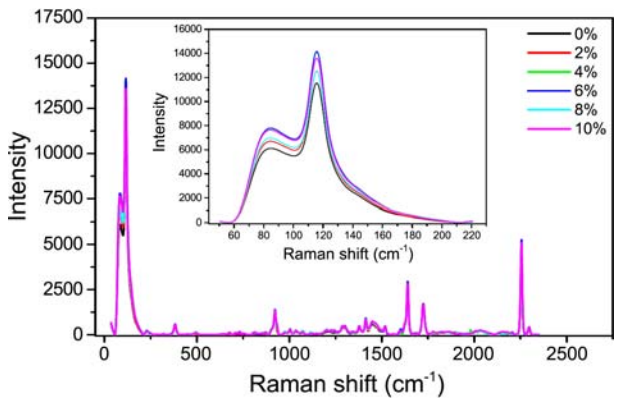

Figure 4. Raman spectra for DSSCs made with a liquid electrolyte and UV-cured resin electrolytes with different GBL concentrations. The inserted is the Raman spectra of the region of the I_3^- species.

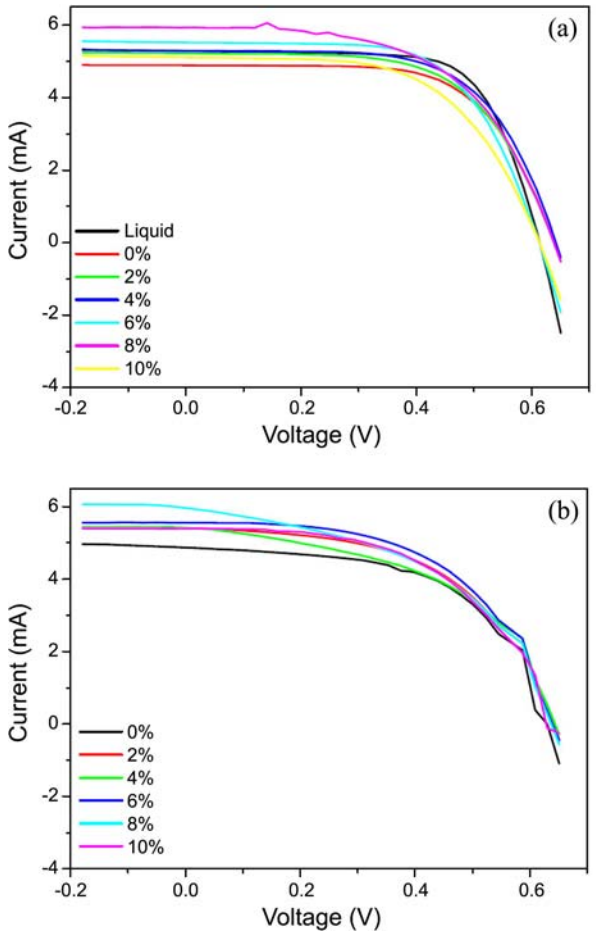

Figure 5. Photocurrent-voltage curves for DSSCs assembled with a liquid electrolyte and UV-cured resin electrolytes with different GBL concentrations before (a) and after (b) UV curing.

electrolytes with different GBL concentrations is very similar to that of the ionic conductivity. This can be explained as the faster diffusion dynamics of the iodide/triiodide species due to the presence of GBL.[21] The intensity of this band is highest with the addition of 6 wt % GBL. This means that the fastest diffusion dynamics of iodide/triiodide species occurs at 6 wt % GBL.

The current-voltage (*I-V*) characteristics were measured under standard AM 1.5G conditions using a 100 mW/cm^2 Xe lamp as the light source. Figure 5(a) shows the *I-V* curves of the DSSCs with the liquid polymer resin electrolytes with different concentrations of GBL before UV curing. The *I-V* curve for the pure-liquid electrolyte is also shown for comparison. The corresponding *I-V* curves for devices with polymer gel electrolytes after UV curing are shown in Figure 5(b). The *I-V* curves for the samples before UV curing have higher short-circuit current density (J_{sc}) than those after UV curing.

The short-circuit current (J_{sc}), open-circuit voltage (V_{oc}), fill factor (FF), corresponding energy conversion efficiency (η) values, and diffusion coefficients (D_{app}) for the polymer resin electrolytes before and after UV curing are summarized in Table 1. The energy conversion efficiency before

Table 1. Diffusion coefficients of I_3^- and the photovoltaic parameters of DSSCs with a liquid electrolyte and with polymer resin electrolytes with different concentrations of GBL before and after UV curing reaction

Condition / Property / Electrolytes	Before UV Curing					After UV Curing				
	V_{oc} (V)	J_{sc} (mA cm^{-2})	D_{app} (cm^2 s^{-1})	*FF* (%)	η (%)	V_{oc} (V)	J_{sc} (mA cm^{-2})	D_{app} (cm^2 s^{-1})	*FF* (%)	η (%)
Liquid	0.61	21.16	1.37	68.92	8.95	-	-	-	-	-
polymer resin with 0% GBL	0.64	19.58	1.27	62.83	7.81	0.62	19.44	1.26	56.01	6.71
polymer resin with 2% GBL	0.65	20.90	1.35	60.43	8.19	0.63	21.63	1.40	52.71	7.23
polymer resin with 4% GBL	0.65	21.23	1.38	61.70	8.48	0.62	21.61	1.40	49.63	6.64
polymer resin with 6% GBL	0.63	22.10	1.43	62.84	8.68	0.62	22.24	1.44	53.73	7.42
polymer resin with 8% GBL	0.66	23.74	1.54	55.21	8.61	0.65	23.77	1.54	47.80	7.45
polymer resin with 10% GBL	0.63	20.44	1.32	58.12	7.43	0.63	21.57	1.40	53.46	7.23

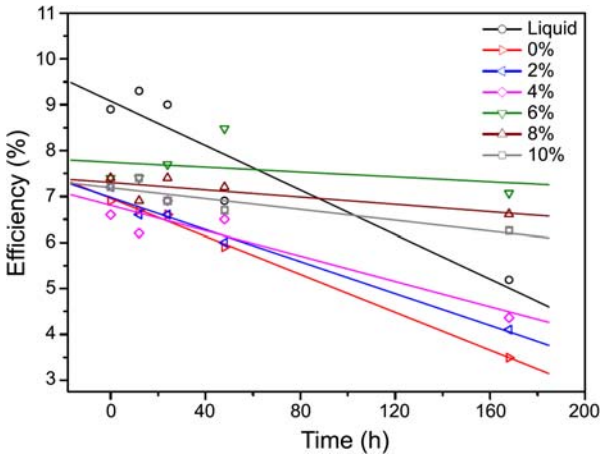

Figure 6. Plot of the conversion efficiencies of the DSSCs assembled with a liquid electrolyte and UV-cured resin electrolytes with different GBL concentrations over time.

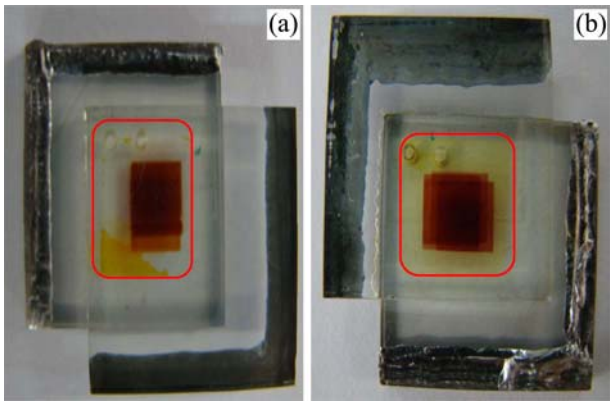

Figure 7. Photos of DSSCs with (a) a liquid electrolyte and (b) a UV-cured resin electrolyte taken 30 days after preparation.

and after UV curing are highest at 6 wt % GBL. The energy conversion efficiency values before UV curing decreased after curing. Interestingly, the decrease in efficiency before and after UV curing at 6 wt % GBL is much less than the decrease in efficiency at other GBL concentrations. This is in good agreement with the results for the ionic conductivity and Raman spectra.

Figure 6 displays the plots of the energy conversion efficiency of the UV-cured DSSCs as a function of time. These indicate the long-term stability of the DSSCs with different concentrations of GBL. The energy conversion efficiency values of all DSSCs decreased with increasing time. However, the energy conversion efficiency of the DSSCs with 6 wt % GBL decreased very slowly, and they were able to maintain higher efficiencies after long periods of time relative to the other devices. This implies that 6 wt % GBL devices are the best for maintaining long-term stability and photovoltaic performance.

Photos of DSSCs with a liquid electrolyte and a UV-cured polymer gel electrolyte taken at 30 days after preparation are provided in Figure 7. The photo of the DSSC with the liquid electrolyte shows leakage and evaporation of the solvent, while that of the UV-cured polymer gel electrolyte DSSC does not show these issues. This shows that the DSSC with the UV-cured polymer gel electrolyte is much more stable than the DSSC with the liquid electrolyte.

Conclusions

We introduced a new UV-cured resin polymer gel as an electrolyte for DSSCs. This new UV-cured resin polymer gel was successfully applied as a gel polymer electrolyte in DSSCs to overcome the issues surrounding liquid electrolytes in DSSCs. GBL was added to the UV-cured resin polymer gel electrolyte to improve the long-term stability and photovoltaic performance of the DSSCs.

The Raman spectra of the UV-cured resin polymer electrolyte with increasing GBL concentrations showed that the intensity of the prominent band observed at 115 cm^{-1}, which is assigned to I_3^-, increased with increasing GBL concentration. This is in good agreement with the ionic conductivity results. The energy conversion efficiency values, ionic conductivity and Raman spectra clearly showed that the addition of 6 wt % GBL to the UV-cured resin polymer electrolyte is the best for the long-term stability and photovoltaic performance of these DSSCs.

Acknowledgments. This work was supported by the National Research Foundation of Korea (NRF) grants funded by the Korea government (MEST) (No. 2009-0087013)

and the BK 21 program from the Ministry of Education, Science and Technology of Korea. The authors thank the Central Laboratory of Kangwon National University for the measurements of Raman spectra.

References

1. O'Regan, B.; Gratzel, M. *Nature* **1991**, *353*, 737.
2. Li, B.; Wang, L.; Kang, B.; Wang, P.; Qiu, Y. *Sol. Energy Mater. Sol. Cells* **2006**, *90*, 549.
3. Mor, G. K.; Varghese, O. K.; Paulose, M.; Shankar, K.; Grimes, C. A. *Sol. Energy Mater. Sol. Cells* **2006**, *90*, 2011.
4. Gratzel, M. *Actual. Chim.* **2007**, *308*, 57.
5. Wang, Y. *Sol. Energy Mater. Sol. Cells* **2009**, *93*, 1167.
6. Park, Y.; Jung, Y. M.; Sarker, S.; Lee, J.-J.; Lee, Y.; Lee, K.; Oh, J. J.; Joo, S.-W. *Sol. Energy Mater. Sol. Cells* **2010**, *94*, 857.
7. Nakade, S.; Kanzaki, T.; Kambe, S.; Wada, Y.; Yanagida, S. *Langmuir* **2005**, *21*, 11414.
8. Reynal, A.; Forneli, A.; Eugenia, M. F.; Antonio, S. D.; Antón, V. F.; Brian, C. O.; Emilio, P. *J. Am. Chem. Soc.* **2008**, *130*, 13558.
9. Kato, N.; Higuchi, K.; Tanaka, H.; Nakajima, J.; Sano, T.; Toyoda, T. *Sol. Energy Mater. Sol. Cells* **2011**, *95*, 301.
10. Chen, H. S.; Lue, S. J.; Tung, Y. L.; Cheng, K. W.; Huang, F. Y.; Ho, K. C. J. *Power Sources* **2011**, *196*, 4162.
11. Wang, P.; Zakeeruddin, S. M.; Moser, J. E.; Baker, R. H.; Gratzel, M. *J. Am. Chem. Soc.* **2004**, *126*, 7164.
12. Ito, S.; Zakeeruddin, S. M.; Comte, P.; Liska, P.; Kuang, D.; Gratzel, M. *Nat. Photonics* **2008**, *2*, 693.
13. Bandara, J.; Weerasinghe, H. *Sol. Energy Mater. Sol. Cells* **2005**, *85*, 385.
14. Senadeera, G. K. R.; Kitamura, T.; Wada, Y.; Yanagida, S. *J. Photochem. Photobiol. A Chem.* **2006**, *184*, 234.
15. Kroeze, J. E.; Hirata, N.; Schmidt-Mende, L.; Orizu, C.; Ogier, S. D.; Carr, K.; Gratzel, M.; Durrant, J. R. *Adv. Funct. Mater.* **2006**, *16*, 1832.
16. Kato, T.; Okazaki, A.; Hayase, S. *J. Photochem. Photobiol. A Chem.* **2006**, *179*, 42.
17. Freitas, J. N.; Longo, C.; Nogueira, A. F.; De Paoli, M.-A. *Sol. Energy Mater. Sol. Cells* **2008**, *92*, 1110.
18. Wu, J. H.; Lan, Z.; Lin, J. M.; Huang, M. L.; Hao, S. C.; Sato, T.; Yin, S. *Adv. Mater.* **2007**, *19*, 4006.
19. Freitas, J. N.; Nogueira, A. F.; De Paoli, M.-A. *J. Mater. Chem.* **2009**, *19*, 5279.
20. Ito, B. I.; Freitas, J. N.; De Paoli, M.-A.; Nogueira, A. F. *J. Braz. Chem. Soc.* **2008**, *19*, 688.
21. Benedetti, J. E.; Gonçalves, A. D.; Formiga, A. L. B.; De Paoli, M.-A.; Li, X.; Durrant, J. R.; Nogueira, A. F. *J. Power Sources* **2010**, *195*, 1246.
22. Nogueira, V. C.; Longo, C.; Nogueira, A. F.; Soto-Oviedo, M. A.; De Paoli, M.-A. *J. Photochem. Photobiol. A Chem.* **2006**, *181*, 226.
23. Nogueira, A. F.; Durrant, J. R.; De Paoli, M.-A. *Adv. Mater.* **2001**, *13*, 826.
24. Nakade, S.; Kanzaki, T.; Wada, Y.; Yanagida, S. *Langmuir* **2005**, *21*, 10803.
25. Kato, T.; Okazaki, A.; Hayase, S. *Chem. Commun.* **2005**, 363.
26. Fukui, A.; Komiya, R.; Yamanaka, R.; Islam, A.; Han, L. *Sol. Energy Mater. Sol. Cells* **2006**, *90*, 649.
27. Lee, C. P.; Lin, L. Y.; Vittal, R.; Ho, K. C. *J. Power Sources* **2011**, *196*, 1665.
28. Lu, H. L.; Lee, Y. H.; Huang, S. T.; Su, C.; Yang, T. C. K. *Sol. Energy Mater. Sol. Cells* **2011**, *95*, 158.
29. Wood, D. M.; Brailsford, A. D.; Dargan, P. I. *Drug Test. Analysis* **2011**, *3*, 417.
30. Zhoua, Y.; Xianga, W.; Chena, S.; Fanga, S.; Zhoua, X.; Zhanga, J.; Lin, Y. *Electrochimica Acta* **2009**, *54*, 6645.